Coverage and temperature-dependent behavior of potassium on Pd{110}

S. J. Pratt, D. K. Escott, and D. A. King*
Department of Chemistry, University of Cambridge, Lensfield Road, Cambridge CB2 1EW, United Kingdom
(Received 20 December 2002; revised manuscript received 7 July 2003; published 11 December 2003)

The adsorption of potassium on Pd{110} has been examined via correlated Auger electron spectroscopy, temperature programmed desorption, low-energy electron diffraction, and secondary electron emission crystal current measurements. Potassium overlayers are disordered at all coverages above 115 K. The uptake of K is readily monitored and the coverage calibrated by measuring the crystal current on adsorption below 200 K. The desorption of multilayer K is found to overlap the low-temperature first layer desorption feature and thus it is not appropriate to assume that the heat of adsorption for first layer K is considerably higher than for multilayer K in this case. Crystal current measurements at higher temperature indicate that some multilayer adsorption sites are populated before the first K layer is saturated. These results reflect the equilibrium distribution of adsorbates over the available sites, which is largely governed by the coverage-dependent differential heats of adsorption for first and second layers.

DOI: 10.1103/PhysRevB.68.235406 PACS number(s): 79.20.Hx, 68.35.Md, 79.20.Fv, 68.43.Vx

I. INTRODUCTION

The bonding of alkali metals with transition metal surfaces is strongly coverage (θ) dependent giving rise to a large temperature range of desorption as demonstrated for the low index planes of Ni (Ref. 1) and a characteristic work function profile like that reported for K on Pd{100}.[2] As discussed in the latest of numerous reviews in this field[3–5] and references therein, alkali adsorption on transition metals has been described by the Langmuir-Gurney model as ionic at low coverage with a gradual transition towards ''metallic'' at saturation.[6,7] Within this model, the adsorption of such an electropositive species results in partial charge transfer from the adsorbate to the substrate and the induced dipole decreases the work function. At low coverage the fall in work function is approximately linear, but at higher coverage where adsorbate interactions become significant, mutual depolarisation results in a work function minimum. The work function smoothly tends towards the value of the bulk alkali at or just beyond completion of a saturated overlayer. Developed in the 1930s, this picture was generally accepted for decades, but in the last 20 years, practical and numerical experiments have highlighted phenomena that are not predicted by the model.[5] They include a range of alkali adsorption sites, only weak coverage dependence of the alkali-substrate bondlength and, for some systems, ''condensation'' of the adlayer into two-dimensional islands of commensurate phases rather than uniform compression with increasing coverage. Such observations have invited renewed interest since the Langmuir-Gurney model is somewhat deficient. Studies examining the electron density calculated using density-functional theory (DFT) have provided further insight into the complex adsorption interaction, and for Co($10\bar{1}0$)-$c(2\times2)$-K the bonding has both ionic and metallic contributions.[8]

Alkalis have been found to induce missing row (MR) reconstruction of a range of fcc {110} surfaces[9–11] and this has been the focus for several investigations of alkali adsorption on Pd{110} to date.[12–14] Barnes *et al.* report low optimal coverages of 0.09 monolayer (ML) Cs and 0.21 ML Na for the (1×2) low-energy electron diffraction (LEED) pattern associated with the MR reconstructed Pd{110} substrate.[12] Like the MR reconstructed Pd{110}-$c(2\times4)$-O structure, the alkali-induced reconstruction is activated and annealing at $\sim$550 K is necessary to obtain good order. Here we present Auger electron spectroscopy (AES), crystal current, and temperature programmed desorption (TPD) measurements characterizing K adsorption on Pd{110} at temperatures below 400 K under which conditions the missing row reconstruction *does not* proceed. These results highlight subtleties in the coverage-dependent heat of adsorption and pinpoint the role of second layer adsorption sites in the uptake of K. Further work examining the coadsorption and reactions of K with CO and CO_2 on this surface has been reported elsewhere.[15]

II. EXPERIMENT

The ultrahigh vacuum (UHV) system in which the experiments were performed has been described in detail previously.[16,17] The Pd crystal (Metal Crystals and Oxides Ltd.) of dimensions $17\times10\times1$ mm was oriented to within 0.5° of the {110} plane and mechanically polished to a mirror finish. Before each experiment the crystal was sputtered with Ar^+ at a surface temperature of 650 K and subsequently annealed at 900 K in 2×10^{-8} mbar O_2 for 30 min. Further heating under UHV to 1000 K induced complete recombinative desorption of $O_{(a)}$ as judged by TPD. Following this treatment the crystal exhibited an Auger spectrum characteristic of Pd and a sharp (1×1) LEED pattern at 360 K. A Pd{110}-$c(2\times4)$-O structure with $\theta_O=0.5$ ML could be prepared by the adsorption of 4 L O_2 at 550 K. The TPD spectrum from this structure exhibited an intense O_2 peak alone and was regularly used to further verify surface cleanliness. The CO and CO_2 features at $T>600$ K, which are readily detected from a very contaminated substrate, were not observed.

Potassium was dosed at normal incidence (towards the front crystal face only) using a resistively heated alkali source (SAES getters), which was positioned at a distance of

60 mm from the sample. After thorough degassing, the chamber pressure rise during source operation was reduced to less than 1.5×10^{-10} mbar and dominated by hydrogen. Time-dependent mass spectra were acquired to monitor the relative K flux while dosing. The K exposure was approximately proportional to the dose time; however, the exposure scale has been normalized to correct for flux variations during the dosing period.

Auger electron spectroscopy or crystal current measurements were performed *in situ* to monitor K adsorption. For AES, the sample potential was modulated and the hemispherical analyzer (VSW HA50) signal demodulated with a lock-in amplifier in order to directly obtain the derivative of the electron energy distribution, $dN(E)/dE$. Crystal current measurements were made with a multimeter (Thurlby Thandar 1906) interfaced with a personal computer and plotted in real time. The high sensitivity of this instrument (1 nA) permitted operation of the electron gun (VSW EG5) in a low beam current regime, which minimized gun outgassing during alkali dosing. On a daily basis, the electron gun was set up to produce a clean surface crystal current of just 0.2 μA with an incidence angle of 45° (filament current 2.2 A, beam energy 300 eV). We found no evidence of electron-stimulated K desorption during Auger or crystal current measurements.

III. RESULTS

A. LEED

We found no K-induced LEED patterns between 115 and 600 K other than the (1×2), which forms on annealing a K-presaturated surface to 550 K, briefly preceded by a (1×3) pattern, and is associated with the missing row reconstruction. Surprisingly, adsorption of K on the well-ordered clean surface at temperatures between 115 and 320 K led to an increasingly bright background and the (1×1) substrate pattern became diffuse, indicating a disordered adlayer. This finding contrasts with the tendency of K to order on other low index Pd substrates and implies structure sensitive behavior. On Pd{100}, $p(2\times2)$ ($\theta=0.25$ ML) and $c(2\times2)$ ($\theta=0.5$ ML) structures are stable to 250 and 300 K, respectively.[2] Similarly the $(\sqrt{3}\times\sqrt{3})R30°$ adlayer found on Pd{111} at 0.33 ML is reported to be stable to at least 200 K.[18]

Following examination of the literature to date regarding late transition metal surfaces with similar anisotropic close packed row structures we suggest that Pd{110} belongs to a family including Ni, Cu, Ag, and probably Rh fcc {110} planes. The clean surfaces are unreconstructed and with the exception of Rh, alkalis have been shown to induce missing row reconstruction of the substrate at or above room temperature.[9] The alkali adlayer is disordered under these temperature conditions. Ordered alkali structures have been identified on the unreconstructed Ag, Cu, and Ni substrates at very low temperature.[10] Qualitatively, $c(n\times2)$ patterns exist above a critical coverage, found to be 0.28 ML for K/Ni{110} at 90 K.[19] It is thought that with increasing coverage, continuous uniaxial compression in the $\langle1\bar{1}0\rangle$ direction occurs, since the smoothest potential runs parallel to the close packed rows. Quasihexagonal structures result and at saturation the separation of nearest-neighbor adatoms is typically just less than that in the bulk bcc alkali metal lattice. The saturation coverage of K/Ni{110} is 0.48 ML and the LEED pattern approaches a $c(2\times2)$. Assuming quite reasonably that K/Pd{110} is analogous to K/Ni{110}, thermal disordering dominates at 115 K, the lower limit of the temperature window accessible with our existing experimental setup. Given that the Pd lattice parameter is 10% larger than that of Ni, a $c(2\times2)$ structure might be expected at 0.5 ML and about 80 K where adsorbate diffusion is suppressed.

Even at high submonolayer coverages this family of unreconstructed fcc {110} surfaces exhibits very low barriers to alkali diffusion in both principal directions, in contrast to a second family of similarly structured planes. On the $\{10\bar{1}0\}$ surfaces of hcp metals, Co and Ru, the $c(2\times2)$-K structure is stable at room temperature.[4,20] Furthermore, these surfaces do not reconstruct following alkali adsorption. Saturation occurs at 0.58 and 0.67 ML for Co and Ru, respectively, and there is strong evidence that beyond 0.5 ML the adlayer is not compressed into an incommensurate phase but rather K atoms are accommodated in asymmetric high-density domain walls.[21] Such a mechanism may prove to be more widely applicable. Finally, of the missing row reconstructed *clean* fcc {110} planes (Pt, Ir, and Au), at room temperature Au{110} exhibits a K-induced (1×3) "double missing row" reconstruction at 0.1 ML and a reconstructed $c(2\times2)$ surface alloy at 0.5 ML, distinct from either family described above.[9]

B. AES at low temperature ($T<200$ K)

The uptake of K could be monitored by following the development of K Auger features or the concomitant attenuation of the Pd peaks, without interrupting the alkali flux. Measurements of the K and Pd Auger signals while dosing K below 200 K were collected in separate experiments. A selection of the raw Auger spectra is shown in Fig. 1.

The relative peak-to-peak height of the principal Pd signal ($M_{4,5}N_{4,5}N_{4,5}$, 329 eV kinetic energy)[22] is plotted as a function of exposure in Fig. 2 (upper trace). There is a marked change in gradient at a relative Auger intensity of 0.62, which is associated with the start of adsorption into second layer sites. It is assumed that the peak-to-peak height of the derivative signal, $dN(E)/dE$, is proportional to the flux of detected electrons for this Auger transition, valid since the peak width is constant (8.5 eV) throughout. A breakpoint in the substrate signal is anticipated if K film growth initially involves adsorption of a saturated overlayer, due to a change in inelastic scattering of the Pd Auger electrons by the K at the onset of second layer growth. Each K atom in the second layer causes a smaller reduction of the substrate AES signal than a K atom in the first layer, giving rise to a shallower Pd signal gradient in the second layer regime. Clearly under these temperature conditions, the transition marking the beginning of second layer adsorption is sharp.

In the absence of any ordered LEED patterns or coverage-dependent sticking probability measurements with which the

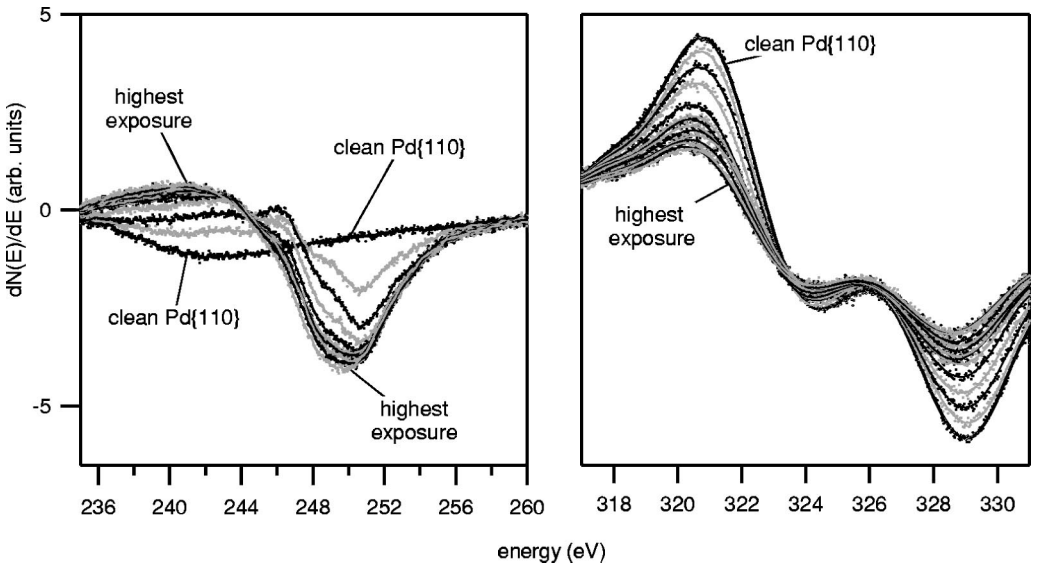

FIG. 1. Attenuation of the principal Pd Auger signal (329 eV) accompanied by growth of the K signal (250 eV) with time while dosing K at $T<200$ K.

K coverage on Pd{110} might be determined, an estimate of the absolute K coverage in monolayers (ML, number of adsorbates per surface atom) at the breakpoint is useful in order to make comparisons with data from other substrates. Should an adsorbed K overlayer be structured like the most dense plane of bulk K, i.e., bcc {110}, it would have a surface atomic density of 5.0×10^{14} cm^{-2}. However, for almost all transition metal substrates, the saturated K overlayer has greater atomic density.[4] Therefore here we suppose the saturated overlayer to be a hexagonally close-packed array of spheres of metallic K of diameter 461 pm, which yields a surface density of 5.59×10^{14} cm^{-2}. In fact this value lies between the experimentally determined saturation coverages for K on Ni{110} (Ref. 19) and Co$\{10\bar{1}0\}$ (Ref. 21) of 5.5×10^{14} cm^{-2} and 5.7×10^{14} cm^{-2}, respectively, and the hexagonally close-packed layer is therefore a sensible choice of model. As the bulk-terminated clean Pd$\{110\}$-(1×1) substrate has a surface density of 9.45×10^{14} cm^{-2}, our model saturated K overlayer with an estimated surface density of 5.59×10^{14} cm^{-2} has a coverage of 0.60 ML. The coverage scale of Fig. 2 is obtained by extrapolation from 0.60 ML at the Pd Auger signal breakpoint, assuming uniform sticking probability. This is thought to be a reasonable assumption since the Auger signal decay with exposure is almost linear. However, it is noted that a 60% drop in K sticking probability on Pt{111} at 0.22 ML has been reported.[23]

The development of the K signal near 250 eV ($L_{2,3}M_{2,3}M_{2,3}$) during dosing below 200 K is also shown in Fig. 1. To extract the relative Auger intensity for the alkali is more of a challenge since the K feature partially overlaps the Pd signal ($M_5N_1N_{4,5}$) at 242 eV, which decays with increasing exposure. Here we used the attenuation and slight shift (-0.9 eV) of the Pd (329 eV) signal with exposure to compute the set of equivalent Pd-derived contributions at 242 eV, which were then subtracted from the raw spectra. Furthermore, the K signal changes energy, shape, and width due to the growth of additional components with increasing exposure (Fig. 1). Thus the relative K Auger intensity is not simply proportional to the peak-to-peak height h, but rather hw^2, where w is the peak width of the $dN(E)/dE$ signal. This relationship assumes a Gaussian peak profile in $N(E)$. The K result is included in Fig. 2 (middle trace) and the change in gradient of the K AES intensity at 0.60 ML is clear. Given the approximations involved we resist the temptation to explore the apparent pre-monolayer break at 0.18 ML. Nevertheless, together the pair of Auger results clearly illustrates the importance of measuring *both* substrate and adsorbate signals in order to make an informed choice of the first layer break and avoid being misled by a pre-monolayer feature.

The expected Auger intensity vs coverage plots for a number of thin-film growth modes have been calculated.[24,25] If core ionization is unaffected by growth of the K layer and elastic scattering is neglected, for idealized Frank–van der Merwe growth (the sequential growth of identical K layers) the substrate Auger intensity is expected to decay with increasing coverage through a series of linear regimes contained within a decaying exponential envelope. The linear dependence arises due to growth of a layer with discrete thickness. Thus in the submonolayer regime, the relative Auger signal, normalized against the clean surface value ($I_{\mathrm{Pd}}/I_{\mathrm{Pd}_0}$) is given by

$$\frac{I_{\mathrm{Pd}}}{I_{\mathrm{Pd}_0}}=(1-x)+x\alpha_K(E), \tag{1}$$

where x is the *fractional* K coverage and $\alpha_K(E)$ the effective transmission factor for Pd Auger electrons of energy E through one K layer. On completion of n layers,

$$\frac{I_{\mathrm{Pd}}}{I_{\mathrm{Pd}_0}}=[\alpha_K(E)]^n. \tag{2}$$

This expression defines the exponential envelope.

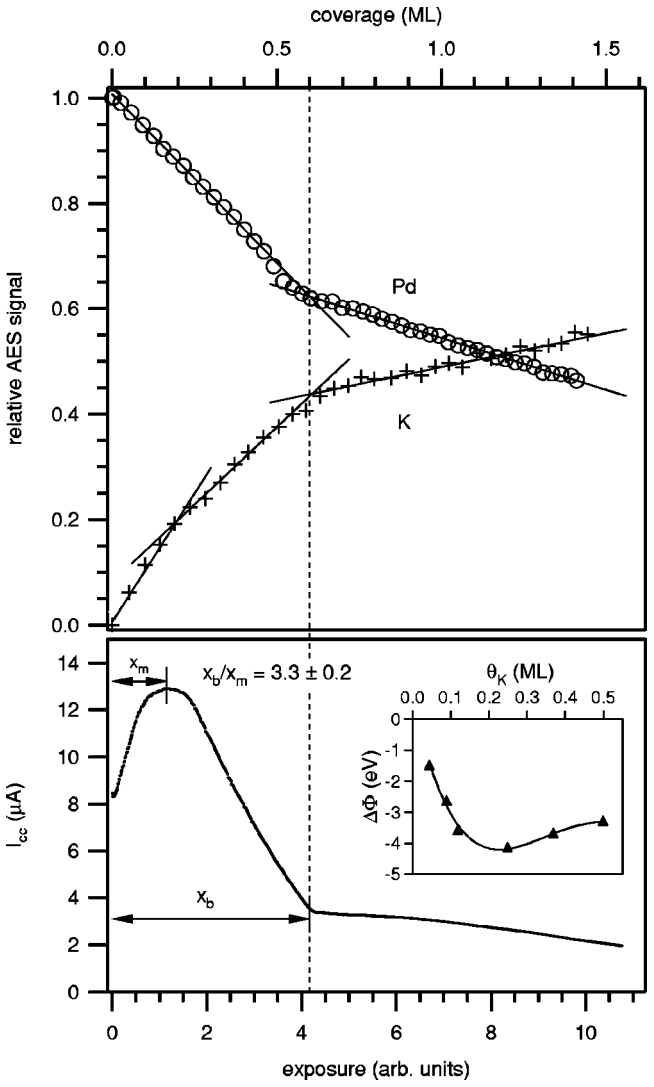

FIG. 2. Exposure dependence of the Pd and K Auger signals [normalized with the clean surface Pd (329 eV) intensity] and the crystal current I_{cc} on dosing K on Pd{110} at $T<200$ K. The coverage scale is determined as discussed in the text. Inset: Coverage dependence of the work function $\Delta\Phi$ for K adsorbed on Pd{100} from Ref. 2.

If the K sticking probability is indeed uniform with coverage, as we have assumed, then the observed linear decay of the Pd Auger signal implies that α_K is constant for coverages <0.48 ML, despite the coverage-dependent changes in adsorbate-substrate bonding. A rational explanation is that the value of α_K is dominated by the total charge density at the surface and is less sensitive to its depth distribution. DFT calculations of Co$\{10\bar{1}0\}$-$c(2\times2)$-K have shown that while in this high coverage structure K can be viewed as donating 0.52 electrons to the substrate, the change in charge density is confined to a region outside the top layer Co cores.[8] Between 0.48 and 0.60 ML the slight dip below the best-fit line implies that the effective transmission factor (α_K) decreases in this coverage regime. This interesting observation may indicate a change in the distribution of electron density at the interface near saturation of the first K layer.

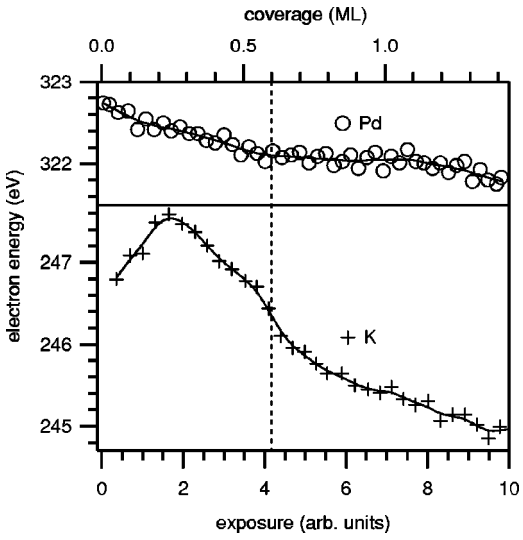

FIG. 3. Exposure dependence of the Pd and K Auger signal energies [peak maxima in the $N(E)$ spectrum], on dosing K at $T<200$ K.

Beyond 0.60 ML, no further breaks were observed, suggesting that thin-film growth is not well described by the Frank–van der Merwe mechanism in this case. The decay has a shallower gradient than the simple model outlined above predicts. Multilayers or crystallites form on top of the first K layer and the observed behavior may well be consistent with the development of a structure that is less dense than the first layer. On metal substrates the first adsorbed layer of K is almost always more dense than bulk K.[4] The declining influence of the substrate on the second or subsequent layers will lead to zero compression of the bulk K structure.

The almost linear behavior of both the Pd and K Auger signal intensities with exposure gives little indication of the coverage-dependent change in chemical state of the alkali from ionic to ''metallic'' evident from the work function behavior. However, integration of the K-derived spectra to obtain $N(E)$ spectra allows the exposure dependence of the peak energy to be determined, as shown in Fig. 3 together with data for the Pd (329 eV) feature. In stark contrast with the Pd signal, which decreases monotonically, the K $(2p,3p,3p)$ peak energy increases reaching a maximum of 247.5 eV at 0.24 ML. The subsequent downshift shows a steeper gradient near 0.60 ML. This coverage-dependent behavior presumably reflects changes in the electronic structure of the K.

C. Crystal current (I_{cc}) at low temperature ($T<200$ K)

The crystal current (I_{cc}), also commonly termed the secondary electron yield (SEY),[26] or the secondary electron emission crystal current (SEECC),[27] is the drain current between earth and the crystal that flows when an electron beam is incident on the crystal. More formally, it is the difference between the current sum of electrons elastically (primary, I_p) or inelastically (secondary, I_s) scattered towards the chamber walls and the incident beam current (I_0). Increasing the al-

kali coverage (θ) gives a characteristic crystal current response that is dominated by the secondary electron current term $I_s(\theta)$,

$$I_{cc}(\theta) = I_p + I_s(\theta) - I_0. \quad (3)$$

The secondary electron emission coefficient $\delta(E_0)$ is defined as

$$\delta(E_0) = (I_p + I_s)/I_0, \quad (4)$$

such that,

$$I_{cc}(\theta) = I_0[\delta(\theta, E_0) - 1]. \quad (5)$$

The crystal current as a function of K exposure on dosing below 200 K is correlated with the Auger results in Fig. 2 (lower trace). It is clearly a sensitive function of exposure exhibiting two characteristic features: a maximum at x_m and a sharp breakpoint at x_b. Although it was not possible to utilize absolute crystal current values due to difficulties in reproducing and maintaining the incident beam characteristics, the pronounced crystal current features occurred reproducibly. The breakpoint is at 3.3 ± 0.2 times the exposure of the crystal current maximum when K is dosed below 200 K. As this value is independent of the incident electron beam flux, we conclude that coverage-dependent electron-stimulated processes do not occur during the measurement.

The origin of the observed behavior can readily be seen by examining the coverage dependence of the energy distribution of scattered electrons, $N(E)$.[28] Detected electrons must have sufficient energy to overcome the surface potential barrier and escape into the vacuum. An increase in crystal current is observed at low coverage and since the work function is known to decrease in this regime (inset, Fig. 2), the secondary emission coefficient, $\delta(300\ \text{eV})$, for clean Pd{110} must be >1. Indeed this is typical of transition metals and from $\delta(E_0)$ results for Pd it has been reported that $\delta_{max} > 1.3$ where $E_{max} > 250$ eV.[29] The crystal current maximum with exposure mirrors the characteristic minimum in the work function observed for alkalis adsorbed on metal surfaces (inset, Fig. 2). The work function was not measured in this study, but it has been shown previously that the crystal current maximum occurs at a coverage just slightly lower than the work function minimum for K and/or Cs on Al{111},[28] Ag{111},[30] and Cu{100} (Ref. 31) surfaces. Beyond the crystal current maximum, the simple anticorrelation between the crystal current and the work function no longer holds. The crystal current falls steeply since for alkalis, in contrast with transition metals, $\delta_{max} < 1$. Specifically for K, $\delta_{max} = 0.7$ and $E_{max} = 200$ eV.[29] At a K film thickness beyond which the experiment is insensitive to the Pd substrate, a crystal current plateau is expected at a negative value, significantly lower than that of the clean Pd substrate.

As shown in Fig. 2, the sharp breakpoint in crystal current is coincident with the breakpoint in the Pd Auger signal and is clearly an independent characteristic critical change that marks the onset of multilayer K adsorption. Such an abrupt feature in the crystal current highlights the differences in the electron-scattering properties of K and Pd at the vacuum interface. This is exemplified by the difference in their δ_{max} values and is a reminder of the scatter of data points on the ''universal'' escape depth curve for the metal substrates studied to date.[32] The uptake of K was routinely monitored *in situ* via crystal current measurements for all subsequent experiments. Coverages were calculated by using the crystal current maximum or break as reference points and assuming the sticking probability to be uniform over the entire exposure regime.

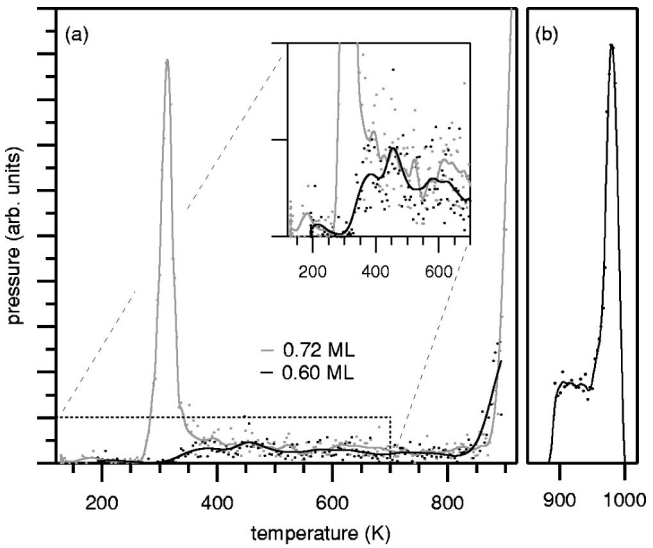

FIG. 4. (a) Potassium (mass 39) desorption obtained on heating at 4 Ks^{-1}. The two solid lines are fits to the raw data points (dots). Traces are shown for a multilayer (0.72 ML, gray) and a layer of approximately 0.60 ML in coverage (black) that was prepared by annealing a multilayer at 311 K. (b) Separate measurement of the high-temperature mass 39 desorption signal. The intensity of the peak at 980 K relative to the multilayer peak at 313 K in (a) is not known.

D. Thermal desorption of K

The strongly coverage-dependent adsorption interaction of K was probed via thermal desorption experiments. As shown in Fig. 4(a) for an initial coverage of 0.72 ML the sharp multilayer desorption at 313 K is readily detectable. Unfortunately, the broad first layer peaks reported previously for K on Pd{110} (Ref. 33) and Pd{100} (Ref. 2) in the temperature range between 400 and 1000 K are close to the sensitivity limit of our experiment and substructure cannot be inferred here. Our TPD sensitivity is low as the mass spectrometer head is located some 150 mm from the sample, such that only a small fraction of the alkali metal desorbing from the crystal is detected. The very intense rise beginning at 880 K has not been reported previously in studies of K desorption from Pd surfaces.[2,33] In contrast to the multilayer feature, the resulting sharp peak at about 980 K shown in Fig. 4(b) is largely insensitive to coverage in the range 0.54–4.20 ML. It is most probably associated with the desorption of K^+ ions[32] which is known to occur if the surface work function is higher than the ionization energy of K (4.34 eV, Ref. 34). As the work function of clean polycrystalline Pd is 5.22 eV,[35] this is possible in a low K coverage regime. Cer-

tainly for K/Pt{111} the efficient detection of such species (ion:neutral sensitivity of 3.4:1) using a Hiden quadrupole mass spectrometer gave rise to an intense and sharp signal at 1100 K.[23] This feature was attributed to deconstruction associated with autocatalytic desorption from subsurface sites. On Pd{110} deconstruction of the K-induced MR (1×2) substrate is observed in LEED after annealing a saturated K overlayer at 785 K for 2 min and is thus complete before the onset of this intense signal.

We can make an estimate for the heat of adsorption at low K coverage since at a desorption peak maximum T_p for first-order desorption,

$$\frac{E_d}{RT_p^2}=\frac{\nu}{\beta}\exp\left(\frac{-E_d}{RT_p}\right), \tag{6}$$

where E_d is the activation energy for desorption, ν the pre-exponential factor, and β the heating rate. This expression is obtained from the Polanyi-Wigner equation[36] for the desorption rate by differentiating and setting $d^2\theta/dt^2=0$ at $T=T_p$.[37] Thus the heat of adsorption (equal to E_d for non-activated adsorption) is approximately 260 kJ mol^{-1} in the zero coverage limit, calculated with $T_p=980$ K for $\beta=4$ Ks^{-1} and assuming that $\nu=10^{13}$ s^{-1}.

The low-temperature regime of Fig. 4 is of primary concern here. A K layer of approximately 0.60 ML in coverage was prepared by dosing 0.72 ML and heating to 311 K for 2 min to desorb the excess K. As shown in the inset of Fig. 4(a), a small but significant pressure associated with K desorption is observed continuously between 315 and 840 K, due to the increase in heat of adsorption with decreasing K coverage. Most significantly, the high coverage submonolayer states are *very* close in desorption temperature to the multilayer peak and there may even be some overlap. There is apparently no temperature window separating them, but experimentalists have frequently assumed the contrary. We will discuss this further in Sec. IV.

Measurements for a range of coverages [Fig. 5(a)] were obtained in order to correlate the multilayer K desorption near 300 K with the crystal current behavior. The higher coverage profiles share their leading edge and the peak maximum shifts to higher temperature with increasing coverage–features that undoubtedly form the zero-order kinetic signature of multilayer desorption. For such systems, the desorption rate is independent of surface coverage since desorption occurs only from sites at the vacuum interface and is given by

$$\frac{-d\theta}{dt}=\frac{-d\theta}{dT}\beta=\nu\exp\left(\frac{-E_d}{RT}\right). \tag{7}$$

Each layer of the multilayer has the same density of sites and thus the coverage of species attempting to desorb remains constant while the multilayer thickness decreases. Consequently, desorption traces for a range of multilayer thicknesses exhibit a common leading edge consistent with the above expression. This is usually true until only the last layer of the multilayer remains, beyond which point the desorption reaction is better described by first-order kinetics and the pressure rapidly falls. From an Arrhenius plot of the leading edge pressure (P) given by the expression (8) below, we obtain an activation energy E_d for multilayer desorption of 75 kJ mol^{-1} and a prefactor of 2.5×10^{12} ML s^{-1} $=82$ ML cm^{-1}.

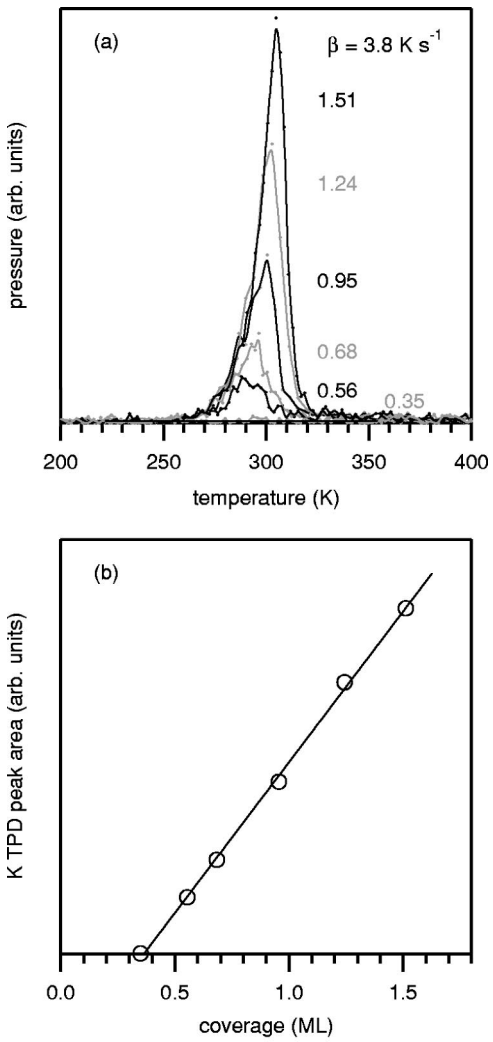

FIG. 5. (a) Desorption (mass 39) near 300 K for a range of initial K coverages from 0.35 to 1.51 ML. (b) Corresponding peak area as a function of coverage.

$$\ln P\propto\ln\left(\frac{-d\theta}{dT}\right)=\frac{-E_d}{RT}+\ln\left(\frac{\nu}{\beta}\right). \tag{8}$$

This crude estimate of E_d is lower than the heat of atomization, reported to be 89.3 kJ mol^{-1}.[34] The pre-exponential factor (ν) can be viewed as the product $\nu=\theta_m\omega$, where θ_m is the coverage of species per layer of the multilayer and ω is close in frequency to the multilayer vibrations characteristic of bonds between the species. With $\theta_m=0.60$ ML, we obtain an ω value of 138 cm^{-1}. Electron energy-loss spectra for K on Pt{111} show that the K mode perpendicular to the surface shifts from 135 cm^{-1} at low coverage to a maximum of 180 cm^{-1} at 0.16 ML K.[38,39] The loss subsequently attenuates and decreases in frequency reaching 155 cm^{-1} at 0.33 ML K. Thus the ω value we determine from the pre-exponential factor is reasonable for a K phonon.

In Fig. 5(b) we present the 300 K desorption peak area plotted against coverage as specified by the crystal current maximum or breakpoint, measured during dosing. In the simplest of models, the K signal at the multilayer desorption temperature is expected to grow linearly above 0.60 ML. However, Fig. 5(b) shows a linear increase above a threshold value of 0.37 ML. The result at 0.56 ML is particularly interesting and shows desorption of K with a peak temperature of 289 K when dosing was terminated before the crystal current break. This indicates that the heat of adsorption is extremely low in the coverage regime $0.37 < \theta_K < 0.60$ ML, such that within this coverage range, first layer K desorption begins at 270 K. For coverages above 0.60 ML the desorption of multilayer K is superimposed on this first layer feature giving rise to a composite signal near 300 K. This result prompted further exploration of the influence of surface temperature on K adsorption.

E. Temperature-dependent features of K adsorption

Without a pulsed resistive heating system, with which Auger or crystal current measurements could be made between heating power pulses while the crystal temperature could be kept constant, experiments were performed while cooling. In Fig. 6(a), raw crystal current data obtained while dosing K on cooling between 350 and 318 K are compared with an analogous experiment between 200 and 140 K. The profiles presented here against time are very similar for $t < 300$ s up to and just beyond the maximum. However, at the higher temperature the crystal current plateaus at about 340 s. As discussed earlier, with the support of Auger data, the crystal current breakpoint at 520 s observed on dosing below 200 K is undoubtedly associated with the onset of multilayer adsorption. The plateau observed at the higher temperature therefore indicates that a steady state is attained at a K coverage of 0.38 ML. Analogous behavior is observed when the adsorption of K near 350 K is tracked by AES as shown in Fig. 6(b). We can use these data to estimate the heat of adsorption at 0.38 ML. At 320 K the rates of adsorption and desorption are equal at the steady-state coverage of 0.38 ML. Therefore if the sticking probability is assumed to be unity, from Fig. 6(a) the incident K flux Z can be calculated and for first-order desorption is also given by

$$Z = \frac{-d\theta}{dt} = \theta \ \nu \exp\left(\frac{-E_d}{RT}\right). \tag{9}$$

Using this expression it is estimated that by 0.38 ML, the heat of adsorption has dropped to $95\ \mathrm{kJ\,mol^{-1}}$ if $\nu = 10^{13}\ \mathrm{s^{-1}}$ is assumed. This is an approximate figure given the assumptions made.

Figure 6(c) includes data from an intermediate temperature range. Qualitatively it is clear that when K is dosed on cooling from 270 K, i.e., below the onset of K desorption, the crystal current break is significantly broadened in comparison with the data below 195 K. As defined by the intersection of two tangents shown in the figure, the break also occurs at a slightly lower exposure such that x_b/x_m is reduced to about 2.7. Broadening of the Pd AES break was also observed under similar temperature conditions, but the effect is more pronounced in the crystal current since it is a stronger function of coverage and shows a bigger change in gradient at 0.60 ML. The broadening is attributed to the population of some multilayer sites at coverages below 0.60 ML, before the first K layer is complete. A substantial temperature-dependent fall in the sticking probability near completion of the first K layer is not expected in this temperature range, below the onset of K desorption.

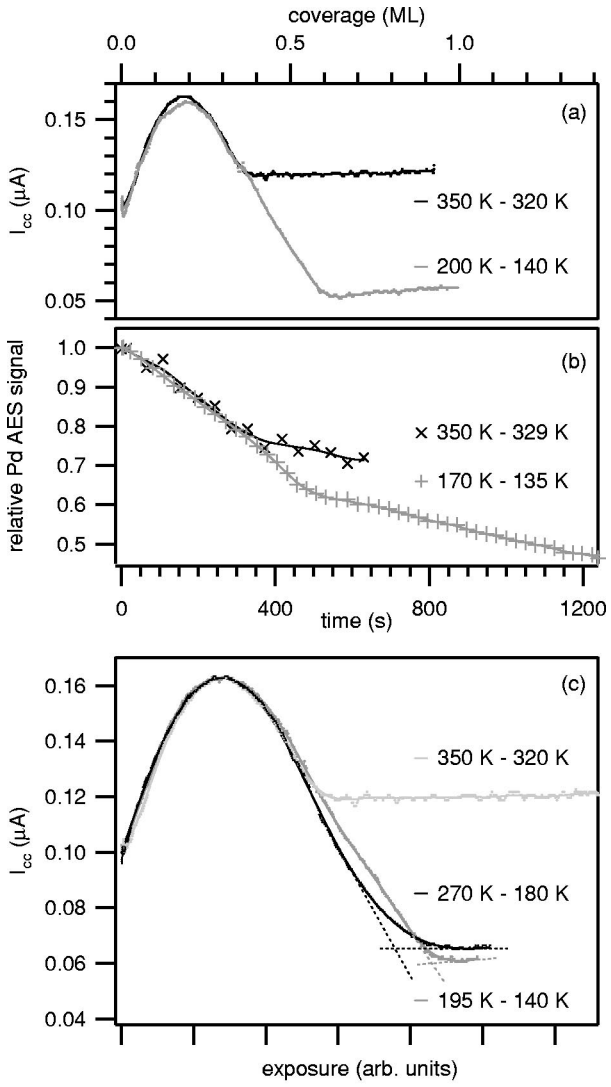

FIG. 6. Effect of adsorption temperature on the crystal current (a) and (c), and Pd Auger signal (b).

IV. DISCUSSION

We believe that broadening of the crystal current break near 0.60 ML is due to a number of K atoms residing in multilayer sites at coverages approaching 0.60 ML. Conditions under which this is possible are now considered. In this coverage regime K adsorption is thought to be precursor mediated. A K atom may initially bind in a second layer site and subsequently diffuse until it finds a vacancy in the first layer that it can occupy. At extremely low temperatures this adsorption mechanism may become kinetically limited by the

rate of diffusion, resulting in a substantial population of atoms in second layer precursor sites. Indeed broadening of Auger breaks in the study of Pb on Cu surfaces has been attributed to diffusion-limited precursor-mediated adsorption.[25] Similarly, for Na on Ni{110},[1] there is evidence in TPD of diffusion-limited adsorption.[40] However, this mechanism is not consistent with the behavior observed in the present study of K on Pd{110}. The absence of ordered K structures on this substrate above 115 K demonstrates that K diffusion is extremely facile at this temperature. Moreover the broadening observed here in the crystal current arises with increasing temperature, whereas diffusion-limited broadening would display the converse temperature dependence.

Therefore the crystal current broadening that we observe must be characteristic of an equilibrated system and thus we turn our attention to the possibility that the population of some multilayer sites becomes thermodynamically favorable at coverages approaching 0.60 ML. The equilibrium distribution of K over the available sites with increasing coverage at a given temperature can be determined if the appropriate thermodynamic parameters are known. Adsorption heats for alkalis on transition metal surfaces have not yet been measured directly via single-crystal adsorption calorimetry (SCAC),[41] so here we present the distribution calculated using schematic coverage-dependent adsorption heats for K on Pd{110} that incorporate the heat values estimated in this work.

For simplicity we neglect the role of sites in the third and subsequent layers in our adsorption scheme. The temperature dependence of the relative adsorption rate into second layer sites with respect to first layer sites at a total coverage θ_T has a Boltzmann form given by

$$\frac{d\theta_2}{d\theta_T}\frac{d\theta_T}{d\theta_1}=\frac{g_2(\theta_2)}{g_1(\theta_1)}\exp\left(\frac{-[q_1(\theta_1)-q_2(\theta_2)]}{\mathrm{RT}}\right). \quad (10)$$

The parameters $q_1(\theta_1)$ and $q_2(\theta_2)$ are the coverage-dependent differential adsorption heats for first and second layer species, respectively. The densities of sites in each layer are denoted $g_1(\theta_1)$ and $g_2(\theta_2)$. The former is $\sim$0.60 ML irrespective of the coverage and as second layer sites are only accessible above occupied first layer sites, we can approximate $g_2(\theta_2)$ as θ_1 for the purpose of this scheme. The values of q at three coverages determined from our K TPD and crystal current results are plotted in Fig. 7. We adopt the value of 75 kJ mol^{-1} in the multilayer regime at 1.5 ML as q_2 and assume this heat to be independent of coverage. While we have just two experimental data points in the low-coverage regime associated with $q_1(\theta_1)$, the breakpoints in Auger and crystal current signals on K adsorption at low temperature confine this parameter to intersect q_2 near 0.60 ML. Note that at the intersection, $d\theta_2/d\theta_1$ becomes unity such that first and second layer sites are filled at the same rate. Furthermore, it is reasonable to invoke an inflexion in $q_1(\theta_1)$ at 0.18 ML because at low coverage the K dipole moment is roughly invariant with coverage and the electrostatic contribution to the bond energy is also invariant. At high coverages, however, as the adlayer becomes ''metallic'' the electrostatic contribution to the adsorption energy is dramatically reduced. Given the exponential form of Eq. (10) the behavior is comparatively insensitive to the differential adsorption heat values when $|q_1(\theta_1)-q_2|$ is $\gg$RT and the inflexion has little influence on the relative adsorption rate. Beyond 0.60 ML, $q_1(\theta_1)$ will drop rapidly when the interactions between nearest neighbors become strongly repulsive, but we have no data for this regime. We thus consider two limiting scenarios labeled A and B in Fig. 7. In A, $q_1(\theta_1)$ falls abruptly at 0.60 ML, whereas it falls slowly with increasing coverage beyond 0.60 ML in B.

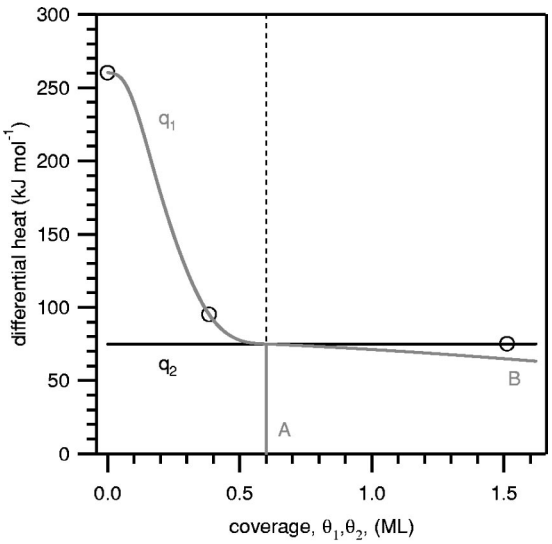

FIG. 7. Heat of adsorption of K/Pd{110} vs coverage. The circles mark values estimated in this work.

Integration of Eq. (10) yields $\theta_2(\theta_1)$ from which $\theta_T(\theta_1)$ can be determined. The resulting coverage distribution with increasing *total* coverage is plotted together with the coverage derivatives for substrate temperatures of 0, 50, and 200 K in Fig. 8. At 0 K (black traces) the first layer coverage (solid line) rises to a saturation value of 0.60 ML at which point the second layer (dotted line) develops exclusively. However, at higher temperature, some second layer sites are thermally populated below 0.60 ML corresponding to the regime where $q_1(\theta_1)$ approaches q_2 before the intersection of Fig. 7. Thus at 200 K (pale gray) θ_2 starts to rise from 0 ML at a total coverage of $\sim$0.5 ML and the transition from first to second layer adsorption is broadened.

In the limit that $q_1(\theta_1)$ falls abruptly at 0.60 ML like A of Fig. 7, θ_1 saturates at 0.60 ML for all temperatures below $\sim$270 K where K begins to desorb. However, in the B limit where $q_1(\theta_1)$ falls slowly beyond 0.60 ML, at finite temperature the first layer coverage further increases and, for example, at 200 K reaches 0.73 ML at a total coverage of 1 ML. Therefore the shaded regions of Fig. 8 show the possible range of behavior between the A and B heat curve limits at 200 K, in which the true $\theta_1(\theta_T)$ and $\theta_2(\theta_T)$ plots will lie. Comparing the traces for 50 and 200 K in the B limit, it is clear that the ''saturation coverage'' of the first adsorbed K layer may vary significantly with surface temperature if the differential heat of adsorption for the first layer above 0.60 ML is close to that of the second layer. As this example

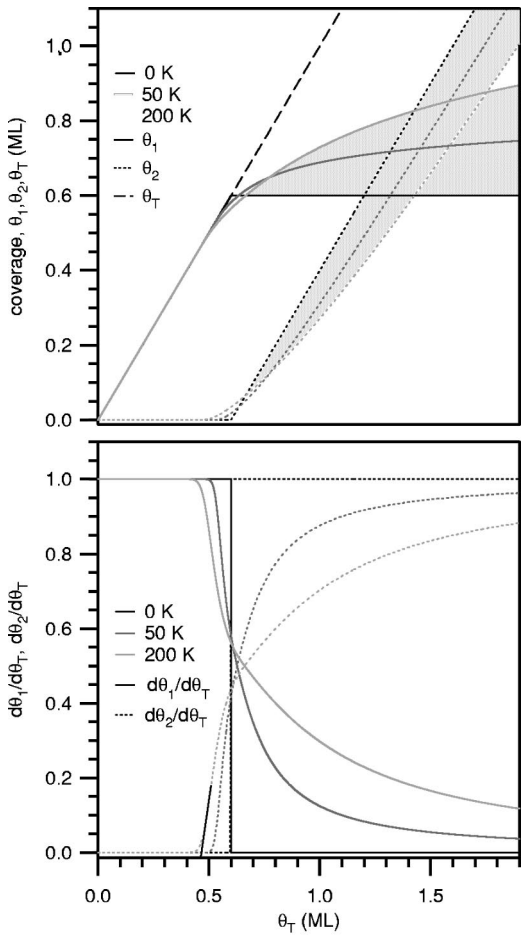

FIG. 8. Schematic distribution of K over first and second layer sites on adsorption at three temperatures. The region spanned at 200 K between the A and B heat curve limits of Fig. 7 is shaded. The corresponding derivatives with total coverage are shown in the lower plot.

illustrates, the saturation coverage of an adsorbate on a given substrate under UHV at a temperature where the desorption rate is negligible is governed by expression (10) for $d\theta_2/d\theta_1$. At 0 K it is simply the coverage at which $q_1(\theta_1)$ and $q_2(\theta_2)$ intersect if $g_1(\theta_1) \approx g_2(\theta_2)$. Note that the formation of a commensurate structure or an adlayer of specific K density/adatom radius are not prerequisites for saturation.

With the aid of Fig. 8, we reconsider the temperature-dependent crystal current measurements of Fig. 6(c) and note that the crystal current break is associated with the start of second layer adsorption rather than the end of adsorption into first layer sites. With increasing temperature the onset of second layer adsorption tends to lower total coverage. This is manifested experimentally as a decrease in the crystal current x_b/x_m ratio from 3.3 at $\sim$150 K to 2.7 at $\sim$200 K. The tangent to $d\theta_2/d\theta_T$ at 200 K included in Fig. 8 pinpoints the onset of second layer adsorption to 0.46 ML. As the crystal current maximum occurs at 0.18 ML, the scheme yields an x_b/x_m ratio of 2.6 at 200 K in excellent agreement with the experimental value.

Assessing the utility of simple techniques to monitor and calibrate alkali adsorption in the absence of ordered structures, several conclusions can be drawn on the basis of this work. Crystal current methods have not been employed previously at temperatures where multilayer growth occurs. We have demonstrated that the onset of multilayer adsorption gives rise to a break in the crystal current with exposure that is very sharp on dosing K below 200 K. The crystal current maximum is a second useful coverage reference and with such ease of implementation this method is preferable to Auger measurements for routine use, necessary since alkali sources age. While the work function exhibits a minimum at a fractional coverage of $\sim$0.5, at high coverage it generally makes a slow approach to the value characteristic of the bulk metal and unlike the crystal current and Auger signals, it shows no distinct change when multilayer adsorption begins. In TPD we have found that a K desorption peak at 290 K corresponding to 0.23 ML first layer atoms overlaps the multilayer desorption signal and thus the onset of the K desorption feature at 290 K is not associated with the onset of multilayer adsorption. Clearly measurements of the crystal current or Auger signals at low temperature are the most reliable methods.

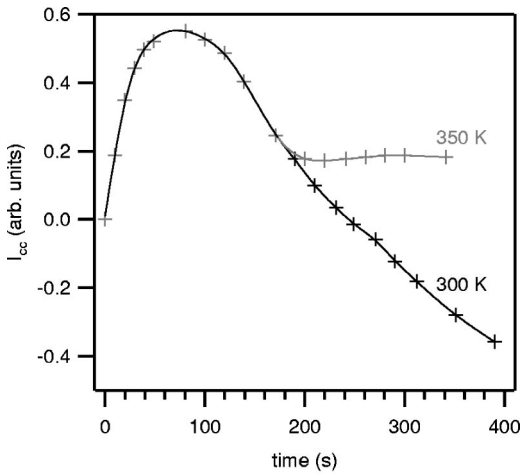

FIG. 9. Crystal current vs deposition time for Na on Pd{110} at 300 and 350 K reported by Barnes (Ref. 26).

It is salient to add that the coverage calibration presented here is at variance with previous studies of alkali adsorption on Pd{110}. Our methodology is strongly supported by an insight into the thermodynamics of K adsorption. Hörnis and Conrad followed the very slow decrease in the Auger K (250 eV): Pd (330 eV) peak-to-peak intensity ratio with time over a period of 10 h at a constant temperature of 470 K.[14] The first break point found in ln(Auger intensity) vs time was attributed to the saturation coverage of 0.60 ML. This cannot be correct, since the TPD spectrum (Fig. 4) indicates that multilayer desorption is complete on heating to 470 K, before the beginning of their measurement.

The exposure-dependent crystal current shown in Fig. 6(a) for K on Pd{110} above room temperature is extremely similar to the profiles measured by Barnes on dosing Na at 350 K or Cs at 300 K.[26] As shown in Fig. 9, when Na is dosed at a slightly lower temperature of 300 K, beyond the maximum the crystal current continues to fall steeply like that obtained on dosing K below 200 K [Fig. 6(a)]. The final

Na exposure is more than five times that of the maximum but for this alkali, the crystal current break must occur at slightly higher exposure. Contrary to the current findings via stringent correlation of the crystal current and Auger experiments probing K uptake, Barnes assumed that the crystal current plateau for Na at 350 K is indicative of a complete first Na layer. However, at this temperature the Na desorption rate is non-negligible in a high coverage regime and the sticking probability falls dramatically before the first layer is filled. Furthermore, the steady state alkali coverage varies strongly with adsorption temperature near 300 K since the heat of adsorption varies only weakly with coverage near 0.60 ML K (Fig. 7). We believe that the coverages reported by Barnes *et al.* for Na on Pd{110}[12,13,26] underestimate the true coverage by at least a factor of 2. Cs coverages are also underestimated.

V. CONCLUSIONS

Coverage calibration of alkali adsorbates on metal substrates is very often achieved by preparing ordered structures of known coverage, which can be detected via LEED. On Pd{110} all coverages of K adlayer are disordered at temperatures above 115 K, precluding that method in this laboratory at present. Below 200 K, a sharp break in secondary electron emission crystal current with K exposure has been found. It is coincident with breakpoints in both the Pd and K Auger signal intensities as functions of K exposure. These observations are associated with a first K layer of approximately 0.60 ML and provide a means of coverage calibration. Coverage-dependent TPD spectra indicate that near 0.60 ML, K desorption signals at 290 K from the first layer and multilayer overlap, which hampers coverage calibration by this technique. We find the crystal current to be a simple but effective monitor of alkali uptake in any coverage regime.

With increasing temperature in the range 200–280 K the crystal current break near 0.60 ML is observed to broaden and to tend towards lower coverage. These effects are due to changes in the equilibrium distribution of K atoms over first layer and multilayer sites with both temperature and coverage. The distribution is predominantly governed by the differential heats of adsorption at first and second layer sites, which are very similar in the coverage regime near 0.60 ML. Consequently, with increasing temperature below 280 K an increasing number of second layer sites are populated before the first layer is saturated. We expect the saturation coverage in the first layer to increase with temperature as a further consequence. Given the strong temperature dependence of the adsorbate distribution over first and second layer sites for K on Pd{110} at 200–280 K, experiments under low-temperature conditions, where first then second layer sites are populated almost sequentially with increasing coverage, are clearly advantageous for coverage calibration purposes. The temperature-dependent behavior observed here in the coverage distribution of K on Pd{110} is highly relevant to many other systems that exhibit bonding lateral interactions at high coverage such as all metals on metal substrates and hydrogen-bonded molecular adsorbates.

ACKNOWLEDGMENTS

We acknowledge financial support for this work from the EPSRC.

*Corresponding author. Fax: +44 1223 762829 (direct), +44 1223 336362 (central); Email address: daksec@ch.cam.ac.uk

[1] R.L. Gerlach and T.N. Rhodin, Surf. Sci. **19**, 403 (1970).
[2] A. Berkó and F. Solymosi, Surf. Sci. **187**, 359 (1987).
[3] M.P. Kiskinova, in *Poisoning and Promotion in Catalysis Based on Surface Science Concepts and Experiments*, edited by B. Delmon and J. Yates, Jr. (Elsevier, Amsterdam, 1992), Vol. 70, p. 19.
[4] R.D. Diehl and R. McGrath, Surf. Sci. Rep. **23**, 43 (1996).
[5] R.D. Diehl and R. McGrath, J. Phys.: Condens. Matter **9**, 951 (1997).
[6] I. Langmuir, J. Am. Chem. Soc. **54**, 2798 (1932).
[7] R.W. Gurney, Phys. Rev. **47**, 479 (1935).
[8] S.J. Jenkins and D.A. King, Chem. Phys. Lett. **317**, 372 (2000).
[9] C.J. Barnes, in *The Chemical Physics of Solid Surfaces*, edited by D.A. King and D.P. Woodruff (Elsevier, Amsterdam, 1994), Vol. 7, p. 501.
[10] R.J. Behm, in *Physics and Chemistry of Alkali Metal Adsorption*, edited by H.P. Bonzel, A.M. Bradshaw, and G. Ertl (Elsevier, Amsterdam, 1989), Vol. 57, p. 111.
[11] C.J. Barnes, M. Lindroos, D.J. Holmes, and D.A. King, in *Physics and Chemistry of Alkali Metal Adsorption* (Ref. 10), p. 129.
[12] C.J. Barnes, M.Q. Ding, M. Lindroos, R.D. Diehl, and D.A. King, Surf. Sci. **162**, 59 (1985).
[13] C.J. Barnes, M. Lindroos, and D.A. King, Surf. Sci. **201**, 108 (1988).
[14] H. Hörnis and E.H. Conrad, Surf. Sci. **322**, 256 (1995).
[15] S.J. Pratt and D.A. King, Surf. Sci. **540**, 185 (2003).
[16] R. Raval, M.A. Harrison, and D.A. King, J. Vac. Sci. Technol. A **9**, 345 (1991).
[17] M.A. Harrison, Ph.D. thesis, University of Liverpool, 1989.
[18] T. Matsushima, J. Phys. Chem. **91**, 6192 (1987).
[19] R.J. Behm, D.K. Flynn, K.D. Jamison, G. Ertl, and P.A. Thiel, Phys. Rev. B **36**, 9267 (1987).
[20] C.J. Barnes, P. Hu, M. Lindroos, and D.A. King, Surf. Sci. **251/252**, 561 (1991).
[21] T. Matsuda, C.J. Barnes, P. Hu, and D.A. King, Surf. Sci. **276**, 122 (1992).
[22] W.A. Coghlan and R.E. Clausing, At. Data **5**, 317 (1973).
[23] J. Lehmann, P. Roos, and E. Bertel, Phys. Rev. B **54**, R2347 (1996).
[24] G.E. Rhead, M.G. Barthès-Labrousse, and C. Argile, Thin Solid Films **82**, 201 (1981).
[25] C. Argile and G.E. Rhead, Surf. Sci. Rep. **10**, 277 (1989).
[26] C.J. Barnes, PhD. thesis, University of Liverpool, 1987.
[27] C. Argile, M.G. Barthès-Labrousse, and G.E. Rhead, Surf. Sci. **138**, 181 (1984).
[28] S.D. Parker and P.J. Dobson, Surf. Sci. **171**, 267 (1986).
[29] A.J. Dekker, in *Solid State Physics*, edited by F. Seitz and D. Turnbull (Academic Press, New York, 1958), Vol. 6, p. 251.
[30] C. Argile and G.E. Rhead, Surf. Sci. **203**, 175 (1988).

[31] C. Argile and G.E. Rhead, Surf. Sci. **279**, 244 (1992).
[32] G.A. Somorjai, *Introduction to Surface Chemistry and Catalysis* (Wiley, New York, 1994).
[33] D. Lackey and D.A. King, J. Chem. Soc., Faraday Trans. 1 **83**, 2001 (1987).
[34] P. Atkins, *Physical Chemistry* (Oxford University Press, Oxford, 1990).
[35] *CRC Handbook of Chemistry and Physics* (CRC Press, Boca Raton, FL, 1999).
[36] D.A. King, Surf. Sci. **47**, 384 (1975).
[37] G.A. Attard and C.J. Barnes, *Surfaces* (Oxford University Press, Oxford, 1998).
[38] J.B. Hannon, M. Giesen, C. Klunker, G.S. IckingKonert, D. Stapel, H. Ibach, and J.E. Muller, Phys. Rev. Lett. **78**, 1094 (1997).
[39] C. Klünker, C. Steimer, J.B. Hannon, M. Giesen, and H. Ibach, Surf. Sci. **420**, 25 (1999).
[40] In Ref. 1, the authors conclude that for Na on Ni{111} and Ni{110} the second Na layer apparently begins to form before the first layer is complete. We question how they have reached this conclusion, as it is not clearly explained. It seems that they assume the desorption peak near 380 K for Na on Ni surfaces to be entirely due to multilayer Na. For Na on Ni{110}, Ref. 1, Fig. 10, this peak starts to develop already at coverage *D*, before the peak near 500 K (the lowest temperature peak that they associate with the first layer) is saturated. This is an example of diffusion-limited adsorption, as equilibrium is not attained at coverage *D*. However, we find for K on Pd{110} through correlated TPD and crystal current measurements that 0.23 ML K atoms adsorbed in the *first* layer desorb at the same temperature as multilayer K. As the saturated first layer coverage is 0.6 ML, this means that more than a third of the first layer atoms desorb at the same temperature as the multilayer. The situation may or may not be similar for Na on Ni and other systems, but in view of our findings, we conclude that the TPD data alone in Ref. 1 cannot reliably indicate the precise coverage at which the Na multilayer begins to form. It is possible that first layer and multilayer Na peaks overlap, as we have found for K on Pd{110}. Thus it is not clear whether it is *second layer* or further *first layer* adsorption that begins before the peak near 500 K is saturated at coverage *D*. The authors of Ref. 1 also suggest (p. 416) that a doublet of peaks in the desorption spectrum of Na from Ni{100} (Fig. 13) is composed of distinct desorption signals from *second* and *third* layer Na atoms. The absence of this feature for Na on Ni{111} and Ni{110} therefore implies that there is not much difference in binding energy of *second* and *third* layer Na on these substrates (not first and second layer Na, as the authors write).
[41] W. Brown, R. Kose, and D.A. King, Chem. Rev. (Washington, D.C.) **98**, 797 (1998).